

Miyake N, Mizuno S, Okamoto N, Ohashi H, Shiina M, Ogata K, Tsurusaki Y, Nakashima M, Saitsu H, Niikawa N, Matsumoto N	KDM6A Point Mutations Cause Kabuki Syndrome	Hum Mutat		Epub ahead of Print	2012
Yamamoto T, Matsuo M, Shimada S, Sangu N, Shimojima K, Aso S, Saito K.	De novo triplication of 11q12.3 in a patient with developmental delay and distinctive facial features.	Mol Cytogenet			in press
Shimada S, Okamoto N, Hirasawa K, Yoshii K, Tani Y, Sugawara M, Shimojima K, Osawa M, Yamamoto T.	Clinical manifestations of Xq28 functional disomy involving MECP2 in one female and two male patients.	Am J Med Genet			in press
Okamoto N, Ohmachi K, Shimada S, Shimojima K, Yamamoto T.	101 kb deletion of chromosome 4p16.3 limited to WHSCR2 in a patient with mild phenotype of Wolf-Hirschhorn syndrome.	Am J Med Genet			in press
Abe Y, Kobayashi S, Wakusawa K, Tanaka S, Inui T, Yamamoto T, Kunishima S, Haginoya K.	Bilateral periventricular nodular heterotopia with megalencephaly: a case report.	J Chil Neurol			in press
Kobayashi S, Inui T, Wakusawa K, Tanaka S, Nakayama T, Uematsu M, Takayanagi M, Yamamoto T, Haginoya K.	A case of atypical benign partial epilepsy with action myoclonus.	Seizure			in press
Okumura A, Hayashi M, Shimojima K, Ikeno M, Uchida T, Takanashi J, Okamoto N, Hisata K, Shoji H, Saito A, Furukawa T, Kishida T, Shimizu T, Yamamoto T.	Whole-exome sequence for a unique brain malformation with periventricular heterotopia, cingulate polymicrogyria, and midbrain tectal hyperplasia.	Neuropathology			in press
Shichiji M, Ito Y, Shimojima K, Nakamu H, Oguni H, Osawa M, Yamamoto T.	A cryptic microdeletion including MBD5 occurring within the breakpoint of a reciprocal translocation between chromosomes 2 and 5 in a patient with developmental delay and obesity.	Am J Med Genet			in press

Okumura A, Shimojima K, Kubota T, Abe S, Yamashita S, Imai K, Okanishi T, Enoki H, Fukasawa T, Tanabe T, Dibbens LM, Shimizu T, Yamamoto T.	PRRT2 mutation In Japanese children with benign infantile epilepsy.	Brain Dev				in press
Shimada S, Okamoto N, Ito M, Arai Y, Momosaki K, Togawa M, Maegaki, Sugawara M, Shimojima K, Osawa M, Yamamoto T.	MECP2 duplication syndrome in both genders.	Brain Dev				in press
Usui D, Shimada S, Shimojima K, Sugawara M, Kawasaki H, Shigematu H, Takahashi Y, Inoue Y, Imai K, Yamamoto T.	Interstitial duplication of 2q32.1-q33.3 in a patient with epilepsy, developmental delay, and autistic behavior.	Am J Med Genet				in press
Shimojima K, Shimada S, Sugawara M, Yoshikawa N, Nijima S, Urao M, Yamamoto T.	Challenges in genetic counseling because of intra-familial phenotypic variation of oral-facial-digital syndrome type 1.	Congenital Anomalies				in press
Okumura A, Hayashi M, Tsurui H, Yamakawa Y, Abe S, Kudo T, Suzuki R, Shimizu T, Yamamoto T.	Lissencephaly with marked ventricular dilation, agenesis of corpus callosum, and cerebellar hypoplasia caused by TUBA1A mutation.	Brain Dev				in press
Miya K, Shimojima K, Sugawara M, Shimada S, Tsurui H, Harai-Tanaka T, Nakaoka S, Kanegane H, Miyawaki T, Yamamoto T.	A de novo interstitial deletion of 8p11.2 including ANK1 identified in a patient with spherocytosis, psychomotor developmental delay, and distinctive facial features.	Gene	506	146-9		2012
Shimojima K, Okamoto N, Suzuki Y, Saito M, Mori M, Yamagata T, Momoi M, Hattori H, Okano Y, Hisata K, Okumura A, Yamamoto T.	Subtelomeric deletions of 1q43q44 and severe brain impairment associated with delayed myelination.	J Hum Genet	57	593-600		2012
Shimojima K, Inoue T, Imai Y, Arai Y, Komoike Y, Sugawara M, Fujita T, Ideguchi H, Yasumoto S, Kanno H, Hirose S, Yamamoto T.	Reduced PLP1 expression in induced pluripotent stem cells derived from a Pelizaeus-Merzbacher disease patient with a partial PLP1 duplication.	J Hum Genet	57	580-586		2012

Shimojima K, Okumura A, Mori H, Abe S, Ikeno M, Shimizu T, Yamamoto T	De novo microdeletion of 5q14.3 excluding MEF2C in a patient with infantile spasms, microcephaly, and agenesis of the corpus callosum.	Am J Med Genet	158A	2272-2276	2012
Shimada S, Miya K, Oda N, Watanabe Y, Kumada T, Sugawara M, Shimojima K, Yamamoto T.	An unmasked mutation of EIF2B2 due to submicroscopic deletion of 14q24.3 in a patient with vanishing white matter disease.	Am J Med Genet	158A	1771-1777	2012
Shimojima K, Mano T, Kashiwagi M, Tanabe T, Sugawara M, Okamoto N, Arai H, Yamamoto T.	Pelizaeus-Merzbacher disease caused by a duplication-inverted triplication-duplication in chromosomal segments including the PLP1 region.	Eur J Med Genet	55	400-403	2012
Nakayama T, Nabatame S, Saito Y, Nakagawa E, Shimojima K, Yamamoto T, Kaneko Y, Okumura K, Fujie H, Uematsu M, Komaki H, Sugai K, Sasaki M.	8p deletion and 9p duplication in two children with electrical status epilepticus in sleep syndrome.	Seizure	21	295-299	2012
Miyatake S, Miyake N, Touho H, Nishimura-Tadaki A, Kondo Y, Okada I, Tsurusaki Y, Doi H, Sakai H, Saitsu H, Shimojima K, Yamamoto T, Higurashi M, Kawahara N, Kawauchi H, Nagasaka K, Okamoto N, Mori T, Koyano S, Kuroiwa Y, Taguri M, Morita S, Matsubara Y, Kure S, Matsumoto N.	Homozygous c.14576G>A variant of RNF213 predicts early-onset and severe form of moyamoya disease.	Neurology	78	803-810	2012
Shimojima K, Okumura A, Natsume J, Aiba K, Kurahashi H, Kubota T, Yokochi K, Yamamoto T.	Spinocerebellar ataxias type 27 derived from a disruption of the fibroblast growth factor 14 gene with mimicking phenotype of paroxysmal non-kinesigenic dyskinesia.	Brain Dev	34	230-233	2012
Shimojima K and Yamamoto T.	Growth profiles of 34 patients with Wolf-Hirschhorn syndrome.	J Pediatr Genet	1	33-37	2012

Takahashi I, Takahashi T, Sawada K, Shimojima K, Yamamoto T.	Jacobsen syndrome due to an unbalanced translocation between 11q23 and 22q11.2 identified at age 40 years.	Am J Med Genet A	158A	220-223	2012
山本俊至	マイクロアレイ染色体検査 の臨床応用	日本小児科学会雑 誌	116	32-39	2012
山本俊至	疾患の責任遺伝子に関する 研究の進歩	脳と発達			in press
川上紀明、辻太一、柳田 晴久、宇野耕吉、松本守 雄、渡辺航太、山元拓哉 、平野徹、種市洋、山崎 健、藤原憲太	肋骨異常を合併した先天性側 弯症：成長期における自然経 過の検討	Journal of Spine Research	3	1470-1474	2012

V. 研究成果の刊行物・別刷

Expression Analysis of a 17p Terminal Deletion, Including *YWHAE*, but not *PAFAH1B1*, Associated With Normal Brain Structure on MRI in a Young Girl

Keisuke Enomoto,^{1,2} Yasuhiro Kishitani,¹ Makiko Tominaga,¹ Aki Ishikawa,¹ Noritaka Furuya,¹ Noriko Aida,³ Mitsuo Masuno,⁴ Ken-Ichiro Yamada,⁵ and Kenji Kurosawa^{1,6*}

¹Division of Medical Genetics, Kanagawa Children's Medical Center, Yokohama, Japan

²Department of Pediatrics and Developmental Biology, Tokyo Medical and Dental University Graduate School of Medical and Dental Science, Tokyo, Japan

³Department of Radiology, Kanagawa Children's Medical Center, Yokohama, Japan

⁴Genetic Counseling Program, Graduate School of Health and Welfare, Kawasaki University of Medical Welfare, Yokohama, Japan

⁵Department of Pediatrics, Hiratsuka City Hospital, Hiratsuka, Japan

⁶Kanagawa Children's Medical Center, Institute for Clinical Research, Yokohama, Japan

Manuscript Received: 28 September 2011; Manuscript Accepted: 1 June 2012

Tyrosine 3-monooxygenase/tryptophan 5-monooxygenase activation protein, epsilon polypeptide (*YWHAE*), on chromosome 17p13.3, has been shown to play a crucial role in neuronal development. The deletion of *YWHAE*, but not platelet-activating factor acetylhydrolase, isoform 1b, subunit 1 (*PAFAH1B1*), underlies a newly recognized neurodevelopmental disorder, characterized by significant growth retardation, developmental delay/intellectual disability (DD/ID), distinctive facial appearance, and brain abnormalities. Here, we report on a girl with a terminal deletion of 17p13.3, including *YWHAE* but not *PAFAH1B1*, showing normal brain structure on MRI. She had mild developmental delay, a distinctive facial appearance, and severe growth retardation despite normal growth hormone levels, which was improved by growth hormone therapy. Expression analysis of *YWHAE* and *PAFAH1B1* yielded results consistent with array CGH and FISH results. These results indicate that the dosage effect of *YWHAE* varies from severe to very mild structural brain abnormalities, and suggest that the expression of *YWHAE* is associated with a complex mechanism of neuronal development. © 2012 Wiley Periodicals, Inc.

Key words: *YWHAE*; *PAFAH1B1*; microdeletion 17p13.3; growth retardation

INTRODUCTION

Deletions of 17p13.3 result in the neuronal migration disorders including lissencephaly and variable structural disorders of the brain [Dobyns et al., 1993]. Haploinsufficiency of platelet-activating factor acetylhydrolase, isoform 1b, subunit 1 (*PAFAH1B1*) and tyrosine 3-monooxygenase/tryptophan 5-monooxygenase activation protein, epsilon polypeptide (*YWHAE*), genes located in this region, are responsible for Miller–Dieker syndrome, which is

How to Cite this Article:

Enomoto K, Kishitani Y, Tominaga M, Ishikawa A, Furuya N, Aida N, Masuno M, Yamada K-I, Kurosawa K. 2012. Expression analysis of a 17p terminal deletion, including *YWHAE*, but not *PAFAH1B1*, associated with normal brain structure on MRI in a young girl.

Am J Med Genet Part A 158A:2347–2352.

characterized by lissencephaly, distinctive facial appearance, and severe neurological dysfunctions [Cardoso et al., 2003].

Recently, it has been shown that patients with deletion of *YWHAE*, but not *PAFAH1B1*, have significant growth retardation, developmental delay/intellectual disability (DD/ID), distinctive facial appearance, and brain abnormalities [Nagamani et al., 2009; Bruno et al., 2010; Mignon-Ravix et al., 2010; Schiff et al., 2010; Shimojima et al., 2010; Tenney et al., 2011]. These results indicated that the *YWHAE* plays a crucial role in neuronal development [Toyo-oka et al., 2003]. The structural abnormalities

Additional supporting information may be found in the online version of this article.

Grant sponsor: The Ministry of Health, Labour and Welfare of Japan.

*Correspondence to:

Kenji Kurosawa, M.D., Ph.D., Division of Medical Genetics, Kanagawa Children's Medical Center, 2-138-4 Mutsukawa, Minami-ku, Yokohama 232-8555, Japan. E-mail: kkurosawa@kcmc.jp

Article first published online in Wiley Online Library (wileyonlinelibrary.com): 7 August 2012

DOI 10.1002/ajmg.a.35542

observed in the brain and cognitive deficiency present in these patients is variable. Recently much attention has been given to the genotype–phenotype correlations based on the breakpoints distal to *PFAFH1B1* in 17p13.3 [Bi et al., 2009].

Here, we report on the case of a girl with mild developmental delay but normal brain structure on MRI, with a terminal deletion of 17p13.3 that involved *YWHAE*, but not *PFAFH1B1*, as demonstrated by FISH and gene expression studies. These results imply that *YWHAE* is associated with a complex mechanism of neuronal development.

CLINICAL REPORT

The 5-year-old girl was born at 40 weeks of gestation by cesarean due to fetal distress, to healthy, non-consanguineous parents. The father and mother were 34 and 33 years old, respectively, and previously had a healthy son. There was no family history of epilepsy and intellectual disability. The girl's birth weight was 2,156 g, length 46 cm, and occipito-frontal circumference (OFC) 33.6 cm, respectively. Her Apgar scores were 6/8. She was hospitalized for severe congenital anemia, caused by feto-maternal transfusion syndrome, and persistent pulmonary hypertension of the newborn.

Developmental milestones were mildly delayed; head control was achieved by 4 months, sitting by 8 months, walking by 18 months, single word by first year, and two-word phrase by 2 years. At 3 years, a ligation procedure for the patent ductus arteriosus was performed. The developmental quotient (DQ), using the Kyoto Scale for Psychological Development, was 70 at the age of 4 years and 9 months. At this age, she presented febrile convulsion lasting 1 min. Biochemical analysis revealed normal levels of insulin-like growth factor-1 (IGF-1), basal growth hormone (GH), thyroid function, cortisol, adrenocorticotropic hormone (ACTH), and prolactin. GH levels in response to stimulation tests were normal for her age. However, growth hormone therapy was started from the age of 4 years as growth retardation had been noted from infancy; this was effective to achieve catch-up growth. Standard karyotyping was normal.

On examination at the age of 5 years, her height was 97.5 cm (−2.4 SD), weight 14.1 kg (−1.5 SD), and OFC 51.4 cm (+0.6 SD). Her facial appearance was distinctive characterized by macrocephaly, a high forehead, hypertelorism, and thin upper lip vermillion (Fig. 1). Brain MRI at 3 T showed almost normal appearances without any structural abnormality but faint patchy high-intensity areas in the frontal subcortical white matter on T2-weighted and fluid attenuated inversion recovery (FLAIR) images (Fig. 2).

MATERIALS AND METHODS

Written informed consent was obtained from the parents of the patient in accordance with the Kanagawa Children's Medical Center Review Board and Ethics Committee.

Molecular Cytogenetic and Array CGH Investigations

An initial FISH analysis for patients with DD/ID and/or multiple congenital anomalies (MCA) was carried out with subtelomeric probes (Vysis, Downers Grove, IL) according to the standard

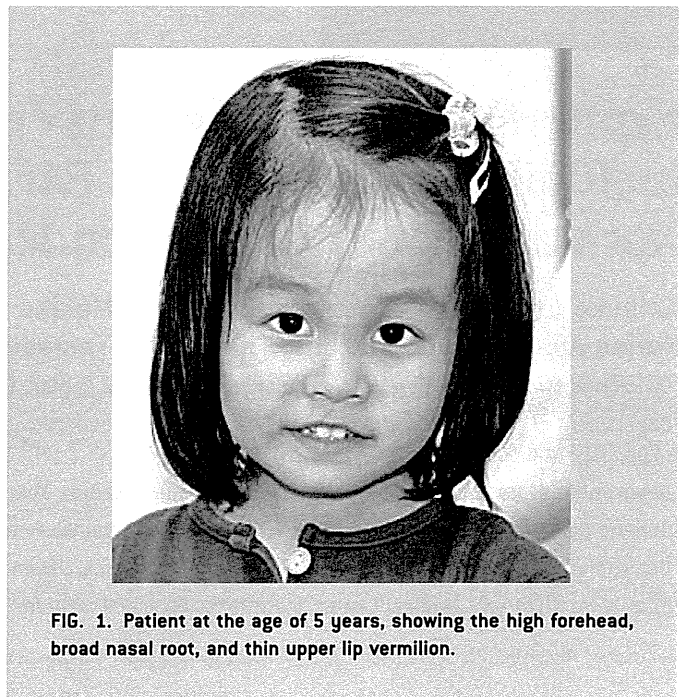


FIG. 1. Patient at the age of 5 years, showing the high forehead, broad nasal root, and thin upper lip vermillion.

protocol. A probe specific for Miller–Dieker syndrome (*LIS1*; Vysis) was also used.

Further FISH analysis for determining the breakpoint on 17p13.3 was carried out using bacterial artificial chromosome (BAC) clones that were selected from the May 2004 (NCBI35/hg17) Assembly of the UCSC Genome Browser (<http://genome.ucsc.edu/>) for Human. A centromere probe for chromosome 17 was used to confirm chromosome 17.

All DNAs were labeled by nick translation, according to the manufacturer's instructions (Vysis). Hybridization, post-hybridization washing, and counterstaining were performed according to standard procedures. Slides were analyzed using a completely motorized epifluorescence microscope (Leica DMRXA2) equipped with CCD camera. Both the camera and microscope were controlled with Leica CW4000 M-FISH software (Leica Microsystems Imaging Solutions, Cambridge, UK) [Yamamoto et al., 2009].

Array-CGH was performed using the Agilent SurePrint G3 Human CGH Microarray Kit 8×60K (Agilent Technologies, Inc., Santa Clara, CA) according to the manufacturer's instructions. The total genomic DNA of the patient was prepared using the standard techniques. The results were analyzed using Agilent Genomic Workbench software. Only experiments having a DLR spread value <0.30 were taken into consideration.

Real-Time PCR

YWHAE is highly conserved and is ubiquitously expressed, but is expressed at highest levels in the brain [Toyo-oka et al., 2003]. To reduce the effects of SNP of *YWHAE* or other genes studied in each subject, we used lymphoblastoid cell lines [Ikeda et al., 2008].

Total RNA from lymphoblastoid cell lines were isolated with the use of a QIAamp RNA Blood Mini Kit (QIAGEN, Valencia, CA).

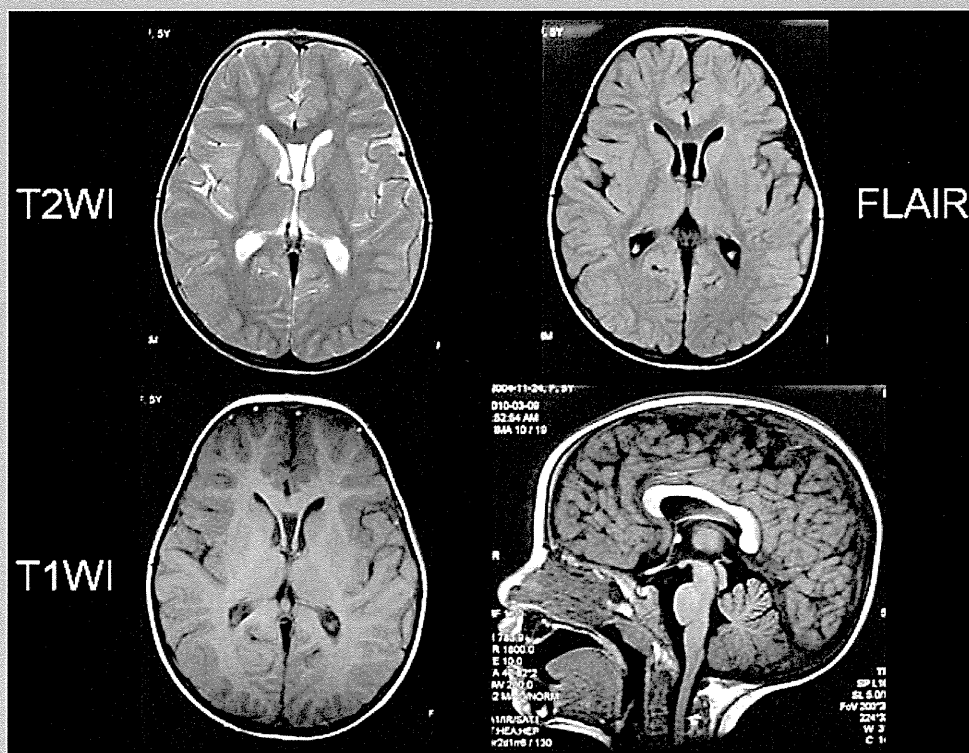


FIG. 2. Brain MRI at the age of 5 years. T1-, T2-weighted, and FLAIR images at 3-Tesla show no clinically significant abnormality but faint patchy high-intensity areas in the frontal subcortical white matter on T2-weighted and FLAIR images.

One microgram of total RNA was used for first-strand cDNA synthesis, using a Transcriptor High Fidelity cDNA synthesis kit (Roche Diagnostics, Rotkreuz, Switzerland). Real-time reverse transcription PCR was performed in a LightCycler 480 (Roche Diagnostics) using SYBR green, under the following cycling conditions: 10 min at 95°C, 45 cycles at 95°C for 30 sec, 60°C for 30 sec, and 72°C for 15 sec. The forward and reverse primer sequences used for *YWHAE* were 5'-GGATACGCTGAGTGAAGAAAGC-3' and 5'-TATTCTGCTCTTCACCGTCACC-3'; for *PFAFH1B1*, primers were 5'-ATGGTCTCTGCTTCAGAGGATG-3' and 5'-GTCATATCTGCAGAACAGGAAGC-3'. Beta-actin was chosen as the reference gene. Statistical analysis was performed using the delta–delta CT method. Lymphoblastoid cell lines from the patient's parents, as well as from a patient with Miller–Dieker syndrome caused by submicroscopic translocation of 17p13.3, including *PFAFH1B1* [Masuno et al., 1995], and from normal females were used for the control materials.

RESULTS

Molecular Cytogenetic and Array CGH Investigations

The complete subtelomere probe set analysis detected a 17pter deletion in the patient. However, the LIS1 probe signal was retained

in the derivative chromosome. To characterize the size of the deletion, we further applied FISH analysis using the BAC clones that mapped to the region (Supplementary eFig. 1—See Supporting Information online). This revealed that the breakpoint was just on the telomeric site of the *PFAFH1B1* gene, about 2.44 Mb from 17pter (Fig. 3). The deleted region included *YWHAE* and *CRK*. Exclusion of mosaicism of the 17pter deletion was confirmed by observation on more than 100 cells.

Subsequent array CGH analysis revealed a 17p13.3 terminal microdeletion of approximately 2.3 Mb in size (chr17: –2,371, 138), which is consistent with the FISH results. No other genomic imbalances were identified on the array analysis. FISH analysis with relevant BAC clones indicated that the translocation was absent in both parents, and therefore had occurred de novo.

Real-Time PCR of *YWHAE* and *PFAFH1B1* mRNA

We compared the expression level of *YWHAE* mRNA between the patient, her parents, a Miller–Dieker syndrome patient, and normal female controls by quantitative real-time PCR (Fig. 4). The relative expression levels were standardized to those of the patient with Miller–Dieker syndrome, which entails haploinsufficiency for both *YWHAE* and *PFAFH1B1*. We found that the *YWHAE* gene expression level in the patient was equal to that in the Miller–Dieker

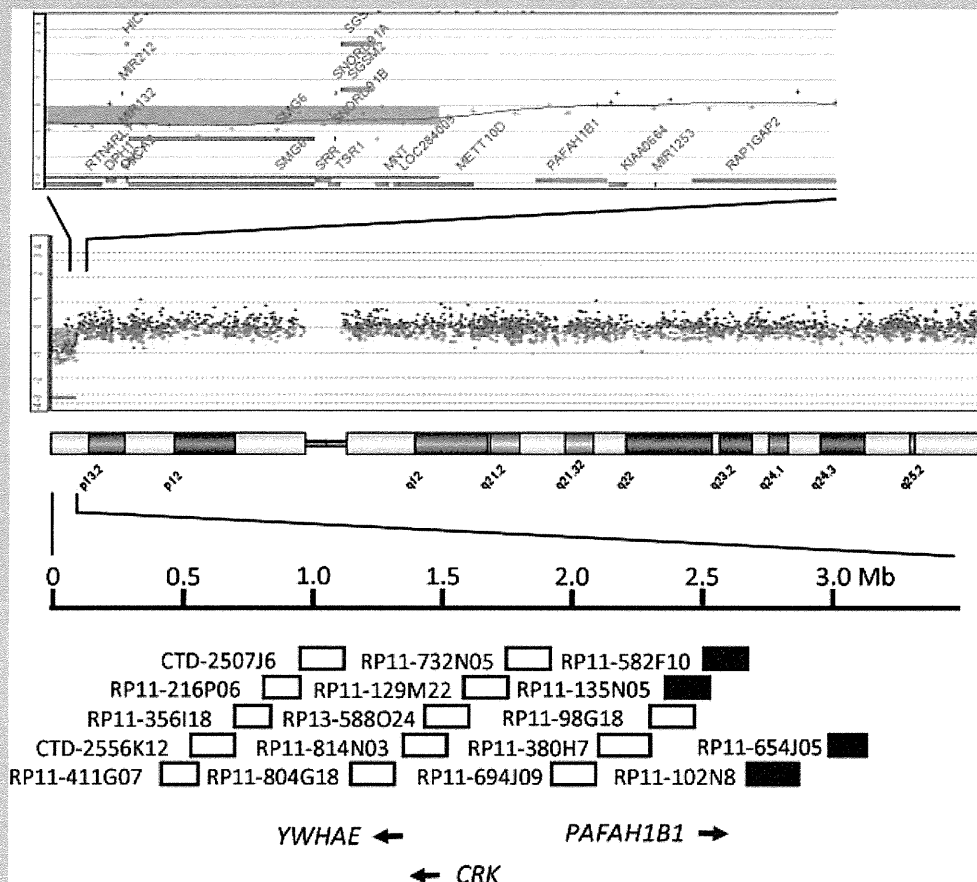


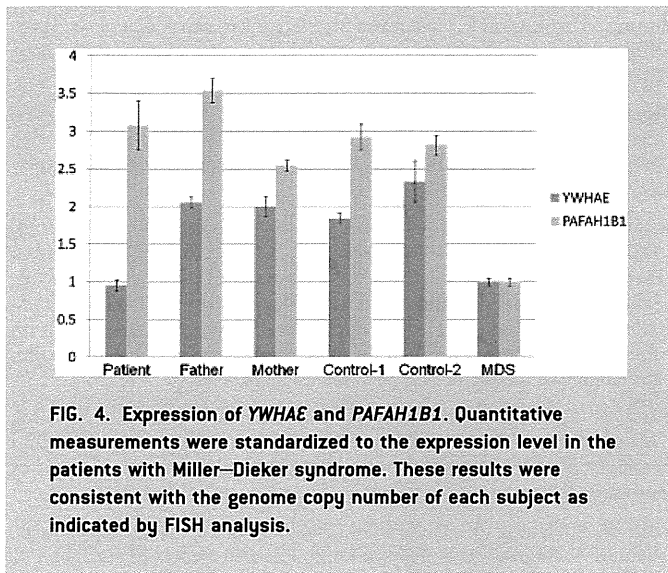
FIG. 3. Schematic representation of 17p13.3 region and bacterial artificial chromosome [BAC] clones used for refinement of the breakpoint derived from the results from array analysis. The map and position of the BAC clones are based on the information from the USCS Genome Browser (Assembly 2004, NCBI35/hg17) and Human 32K BAC Re-Array from Children's Hospital Oakland Research Institute (CHORI) BACPAC Resource. Signal retention was detected at RP11-135N5, but not at RP11-98F18, demonstrating that the breakpoint was just distal from *PAFAH1B1*. The deleted clones are indicated by open boxes, and non-deleted clones by full boxes.

syndrome patient, but was half that of her parents and normal controls. However, the expression level of *PAFAH1B1* in the patient was equal to that of the controls, but was twofold that of Miller–Dieker syndrome patient. These results were consistent with the molecular cytogenetic results.

DISCUSSION

Microdeletion of 17p13.3 involving *YWHAE*, but distal to *PAFAH1B1*, is a newly recognized syndrome associated with variable disorders of cortical development and facial dysmorphism. Here, we describe identification of a terminal microdeletion of 17p13.3 involving the *YWHAE* gene and *CRK* gene but not *PAFAH1B1*, in a girl, who had experienced mild developmental delay, short stature, and had a distinctive facial appearance, but who demonstrated normal cortical development on MRI. Expression

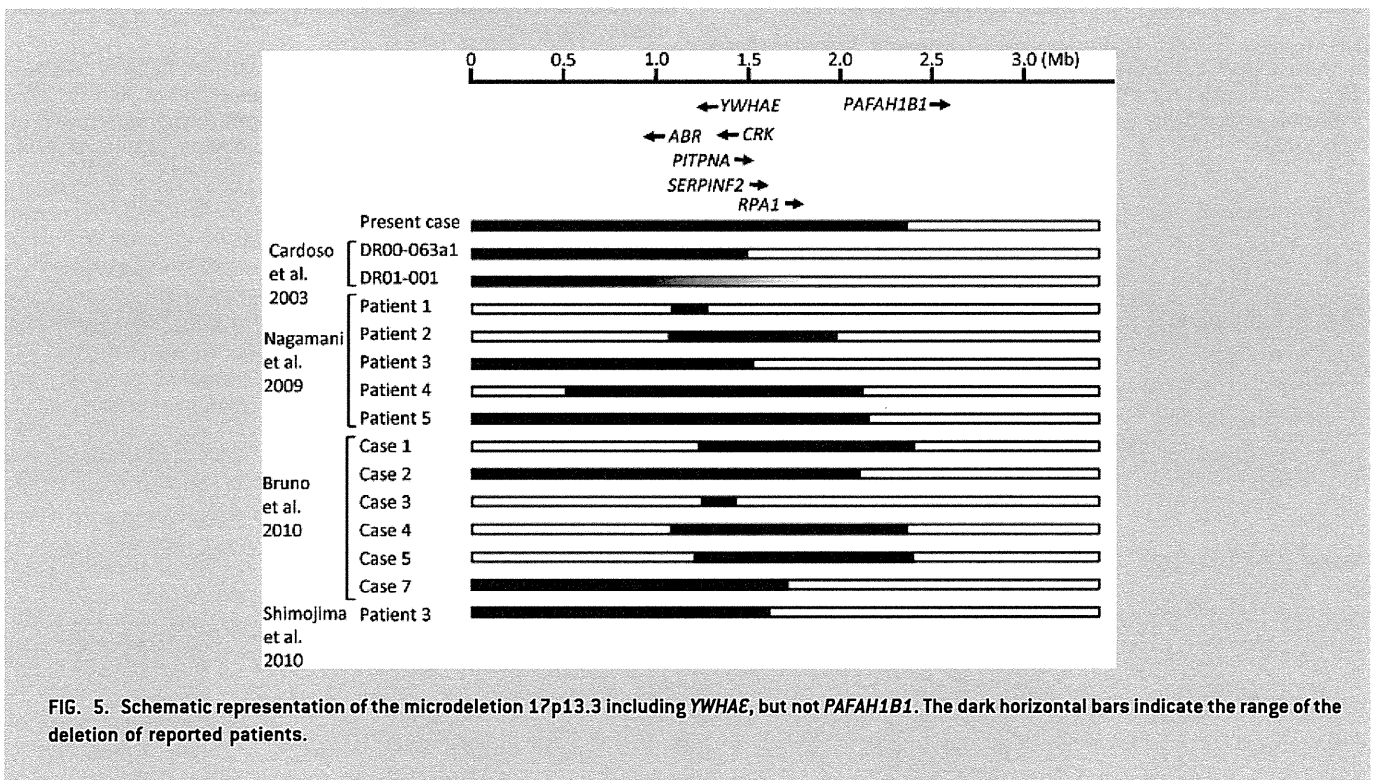
studies of *YWHAE* and *PAFAH1B1* correlated with FISH results. This is the first report of evidence of dosage effects of the *YWHAE* gene in a patient with 17p13.3 microdeletion. *YWHAE* haploinsufficiency results in brain malformation, including cortical defects and corpus callosum hypoplasia, in both mice and humans [Toyooka et al., 2003; Mignon-Ravix et al., 2010]. However, the present case demonstrated normal brain structure on MRI. The structural brain abnormalities in patients with deletion of *YWHAE*, but not *PAFAH1B1*, have been shown to be variable; this variation included normal MRI findings [Nagamani et al., 2009; Bruno et al., 2010; Mignon-Ravix et al., 2010; Schiff et al., 2010; Shimojima et al., 2010; Tenney et al., 2011]. To our knowledge, two other cases with *YWHAE* deletion, but without obvious abnormalities on MRI, have been reported (Case DR00-063a1 in Cardoso et al. [2003], Patient 3 in Nagamani et al. [2009]). The structural variation of the brain and severity of intellectual disability or development



YWHAE has been shown to function within a complex with several other factors, such as *PAFAH1B1* and *NUDEL*. Recently, using the global gene expression and pathway analysis in targeted gene mutations of *Lis1*, *Dcx*, *Ywhae*, and *Ndel1*, Pramparo et al. [2011] demonstrated that cell cycle and synaptogenesis genes are similarly expressed and are co-regulated in the developing brains of normal and mutant mouse in a time-dependent manner. Thus, reduced expression levels of *YWHAE* may still be able to mediate normal brain structure, as detected by MRI in humans [Bruno et al., 2010]. Further analysis of correlation between clinical phenotype and expression levels of related genes in brain development are required for elucidating the mechanism of neurodevelopmental disorders associated with mutations involving *YWHAE*.

The present patient we described here showed prenatal onset of growth retardation, in the absence of growth hormone deficiency; however, growth hormone therapy was effective in mediating catch-up growth from the age of 4 years. Prenatal onset of severe growth retardation is common to patients with deletions of the subtelomeric region of 17p13.3 involving *YWHAE*. However, in those cases with small, limited deletions involving *YWHAE*, growth retardation is not so severe, as seen in Patient 1 reported by Nagamani et al. [2009] and the patient described by Mignon-Ravix et al. [2010]. Therefore, evaluation of hormones associated with growth in patients with a 17p13.3 microdeletion will also provide further insights into the genotype–phenotype correlations attributed to genes involved in these disorders.

represented no strict correlation in the cases with deletion of *YWHAE* but not *PAFAH1B1* (Fig. 5). These results indicated that the *YWHAE* plays a crucial role in neuronal development in humans, but does not result in structural abnormalities of the brain in a haploinsufficiency state. This is in contrast to *PAFAH1B1*; haploinsufficiency of this gene alone contributes to lissencephaly.



ACKNOWLEDGMENTS

We thank the patient and her family for making this study possible. We are also grateful to Dr. Shuki Mizutani (Tokyo Medical and Dental University) and Dr. Hiroyuki Ida (Tokyo Jikei University) for their valuable comments. This research was supported in part by a Grant-in-aid from the Ministry of Health, Labour and Welfare, Japan.

REFERENCES

- Bi W, Sapir T, Shchelochkov OA, Zhang F, Withers MA, Hunter JV, Levy T, Shinder V, Peiffer DA, Gunderson KL, Nezarati MM, Shotts VA, Amato SS, Savage SK, Harris DJ, Day-Salvatore D-L, Horner M, Lu X-Y, Sahoo T, Yanagawa Y, Beaudet AL, Cheung SW, Martinez S, Lupski JR, Reiner O. 2009. Increased LIS1 expression affects human and mouse brain development. *Nat Genet* 41:168–177.
- Bruno DL, Anderlid BM, Lindstrand A, van Ravenswaaij-Arts C, Ganesamoorthy D, Lundin J, Martin CL, Douglas J, Nowak C, Adam MP, Kooy RF, Van der Aa N, Reyniers E, Vandeweyer G, Stolte-Dijkstra I, Dijkhuizen T, Yeung A, Delatycki M, Borgström B, Thelin L, Cardoso C, van Bon B, Pfundt R, de Vries BB, Wallin A, Amor DJ, James PA, Slater HR, Schoumans J. 2010. Further molecular and clinical delineation of co-locating 17p13.3 microdeletions and microduplications that show distinctive phenotypes. *J Med Genet* 47:299–311.
- Cardoso C, Leventer RJ, Ward HL, Toyo-Oka K, Chung J, Gross A, Martin CL, Alanson J, Pills DT, Olney AH, Mutchinick OM, Hirotsune S, Wynshaw-Boris A, Dobyns WB, Ledbetter DH. 2003. Refinement of 400-kb critical region allows genotypic differentiation between isolated lissencephaly, Miller-Dieker syndrome, and other phenotypes secondary to deletions of 17p13.3. *Am J Hum Genet* 72:918–930.
- Dobyns WB, Reiner O, Carrozzo R, Ledbetter DH. 1993. Lissencephaly. A human brain malformation associated with deletion of the LIS1 gene located at chromosome 17p13. *JAMA* 270:2838–2842 (Review).
- Ikeda M, Hikita T, Taya S, Uruguchi-Asaki J, Toyo-oka K, Wynshaw-Boris A, Ujike H, Inada T, Takao K, Miyakawa T, Ozaki N, Kaibuchi K, Iwata N. 2008. Identification of YWHAE, a gene encoding 14-3-3 epsilon, as a possible susceptibility gene for schizophrenia. *Hum Mol Genet* 17:3212–3222.
- Masuno M, Imaizumi K, Nakamura M, Matsui K, Goto A, Kuroki Y. 1995. Miller-Dieker syndrome due to maternal cryptic translocation t(10;17)(q26.3;p13.3). *Am J Med Genet* 59:441–443.
- Mignon-Ravix C, Cacciagli P, El-Waly B, Moncla A, Milh M, Girard N, Chabrol B, Philip N, Villard L. 2010. Deletion of YWHAE in a patient with periventricular heterotopias and pronounced corpus callosum hypoplasia. *J Med Genet* 47:132–136.
- Nagamani SC, Zhang F, Shchelochkov OA, Bi W, Ou Z, Scaglia F, Probst FJ, Shinawi M, Eng C, Hunter JV, Sparagana S, Lagoe E, Fong CT, Pearson M, Doco-Fenzy M, Landais E, Mozelle M, Chinault AC, Patel A, Bacino CA, Sahoo T, Kang SH, Cheung SW, Lupski JR, Stankiewicz P. 2009. Microdeletions including YWHAE in the Miller-Dieker syndrome region on chromosome 17p13.3 result in facial dysmorphisms, growth restriction, and cognitive impairment. *J Med Genet* 46:825–833.
- Pramparo T, Libiger O, Jain S, Li H, Youn YH, Hirotsune S, Schork NJ, Wynshaw-Boris A. 2011. Global developmental gene expression and pathway analysis of normal brain development and mouse models of human neuronal migration defects. *PLoS Genet* 7:e1001331.
- Schiff M, Delahaye A, Andrieux J, Sanlaville D, Vincent-Delorme C, Aboura A, Benzacken B, Bouquillon S, Elmaleh-Berges M, Labalme A, Passemar S, Perrin L, Manouvrier-Hanu S, Edery P, Verloes A, Drunat S. 2010. Further delineation of the 17p13.3 microdeletion involving YWHAE but distal to PAFAH1B1: Four additional patients. *Eur J Med Genet* 53:303–308.
- Shimajima K, Sugiura C, Takahashi H, Ikegami M, Takahashi Y, Ohno K, Matsuo M, Saito K, Yamamoto T. 2010. Genomic copy number variations at 17p13.3 and epileptogenesis. *Epilepsy Res* 89:303–309.
- Tenney JR, Hopkin RJ, Schapiro MB. 2011. Deletion of 14-3-3{varepsilon} and CRK: A clinical syndrome with macrocephaly. Developmental delay, and generalized epilepsy. *J Child Neurol* 26:223–227.
- Toyo-oka K, Shionoya A, Gambello MJ, Cardoso C, Leventer R, Ward HL, Ayala R, Tsai LH, Dobyns W, Ledbetter D, Hirotsune S, Wynshaw-Boris A. 2003. 14-3-3 Epsilon is important for neuronal migration by binding to NUDEL: A molecular explanation for Miller-Dieker syndrome. *Nat Genet* 34:274–285.
- Yamamoto K, Yoshihashi H, Furuya N, Adachi M, Ito S, Tanaka Y, Masuno M, Chiyo H, Kurosawa K. 2009. Further delineation of 9q22 deletion syndrome associated with basal cell nevus (Gorlin) syndrome: Report of two cases and review of the literature. *Congenit Anom (Kyoto)* 49:8–14.

A case of Sjögren-Larsson syndrome with minimal MR imaging findings facilitated by proton spectroscopy

Yasuhiko Tachibana · Noriko Aida · Keisuke Enomoto · Mizue Iai · Kenji Kurosawa

Received: 7 March 2011 / Revised: 2 May 2011 / Accepted: 6 May 2011 / Published online: 29 June 2011
© Springer-Verlag 2011

Abstract We present a 5-year-old girl who was ultimately diagnosed with Sjögren-Larsson syndrome (SLS). Although her MRI findings were minimal compared to previously published cases, prominent and characteristic abnormal lipid peaks on single-voxel proton MR spectroscopy (^1H -MRS) facilitated the diagnosis. This case emphasizes the importance and usefulness of ^1H -MRS in diagnosing SLS.

Keywords Sjögren-Larsson syndrome · MR spectroscopy · Lipids · Molecular study

Introduction

Sjögren-Larsson syndrome (SLS) is a rare autosomal-recessive neurocutaneous disorder characterized by a clinical triad of congenital ichthyosis, spastic diplegia or tetraplegia and mental retardation. The symptoms may be apparent at birth, and the syndrome usually develops in the first years of life [1]. The severity of the symptoms is variable and a few cases have very mild symptoms [2];

however, some hyperkeratosis seems inevitable. SLS is caused by deficiency of the microsomal enzyme fatty aldehyde dehydrogenase (FALDH) due to mutations in the *ALDH3A2* gene [3]. This results in accumulation of fatty alcohols, modification of macromolecules by fatty aldehydes and the presence of high concentrations of biologically active lipids, which have been postulated to be the pathophysiological mechanism of symptoms in SLS [1]. Previous studies regarding proton MR spectroscopy (^1H -MRS) of the brain in SLS patients have revealed abnormal lipid peaks at 1.3 ppm and/or 0.9 ppm [1], in addition to the characteristic MRI findings including a zone of abnormal high signal intensity in the periventricular white matter on T2-weighted images and delayed myelination development [1].

We present a girl with SLS whose brain MRI findings were minimal and nonspecific but who had prominent lipid peaks on ^1H -MRS. The suspicion of SLS was facilitated by this finding on ^1H -MRS in addition to her clinical symptoms. A distinct diagnosis based on a molecular analysis of her *ALDH3A2* gene was made.

Case report

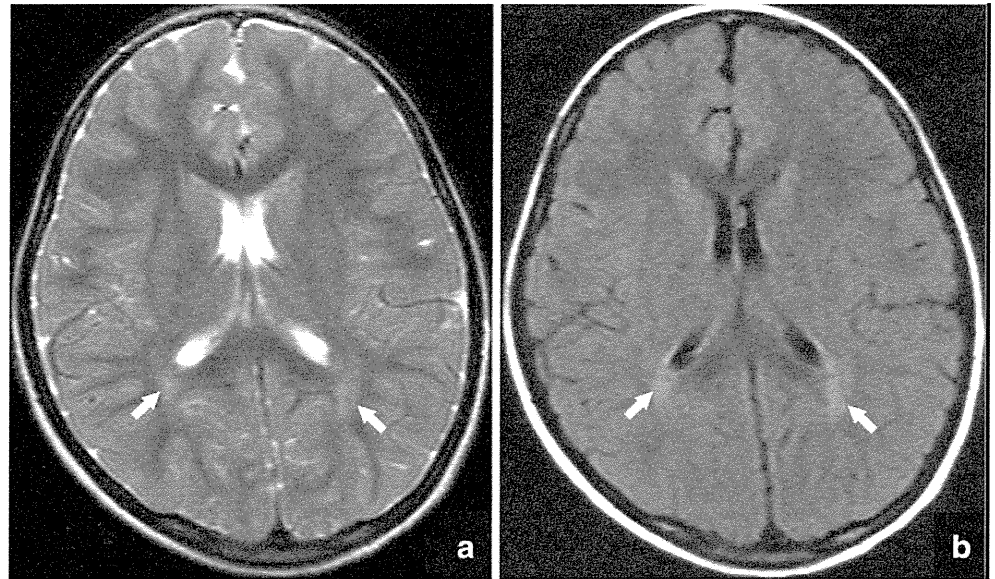
The girl, born at 39 weeks' gestation to unrelated healthy parents, was 5 years old when she underwent MRI/ ^1H -MRS examination to evaluate unexplained lower limb spasticity. Her skin was normal in her first months of life, but hyperkeratosis on her trunk and limbs appeared in her first year of life, and developed into acanthosis and ichthyosis in the next year. However, SLS was not considered at the time. Her motor development was mildly delayed, with her achieving head control at 4 months, rolling over at 6 months, crawling at 12 months and walking without support at 21 months of age. She had a spastic gait with

Y. Tachibana (✉) · N. Aida
Department of Radiology, Kanagawa Children's Medical Center,
2-138-4 Mutsukawa, Minami-ku,
Yokohama, 232-8555, Japan
e-mail: yaz.tachibana@radio.email.ne.jp

K. Enomoto · K. Kurosawa
Division of Medical Genetics,
Kanagawa Children's Medical Center,
Yokohama, Japan

M. Iai
Department of Neurology, Kanagawa Children's Medical Center,
Yokohama, Japan

Fig. 1 MRI findings. **a** T2-weighted image (TR/TE=3,880/119 msec) and **(b)** T2-weighted fluid-attenuated inversion recovery image (TR/TE/TI=9,000/116/2,406 msec). The minimal high-intensity lesions in the deep white matter around the trigones of the bilateral lateral ventricles are scarcely distinguishable from a normal nonmyelinated lesion considering her age (*arrows*). TR = repetition time, TE = echo time, TI = inversion time



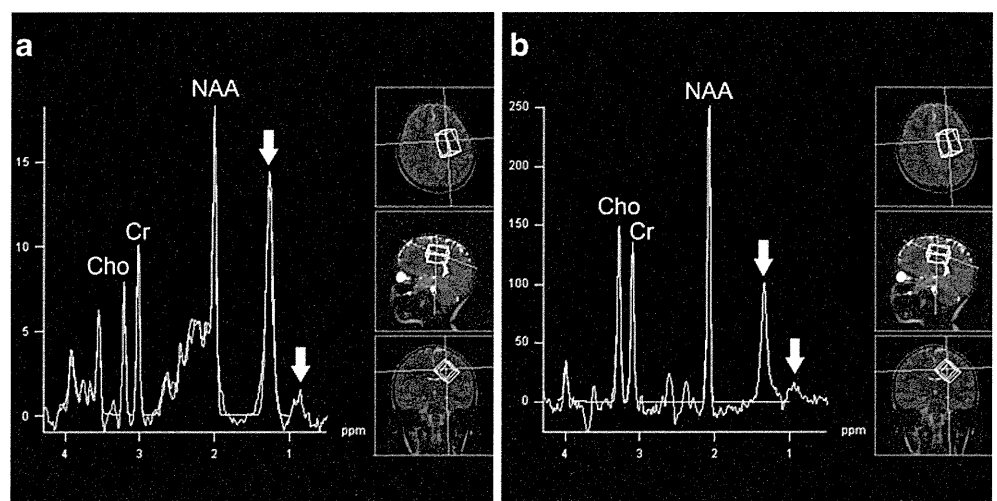
brisk deep tendon reflexes in her bilateral lower limbs, and developed worsening spasticity during her first 2 years. She had no deficiencies in intellectual development.

MR examinations were performed on a 1.5-T MRI system (Siemens MAGNETOM Avanto, Siemens Medical Solutions, Erlangen, Germany), by using a 12-channel head coil. ¹H-MRS was added to the MRI brain imaging sequences (i.e. transverse and sagittal T1-weighted spin-echo imaging, transverse and coronal T2-weighted fast spin-echo imaging, transverse diffusion-weighted imaging, and T2-weighted fluid-attenuated inversion recovery imaging (FLAIR), as is routinely done at our clinics when patients have neurological findings as in this case. ¹H-MRS was acquired by the single-voxel point resolved spectroscopy (PRESS) sequence. Repetition time (TR), echo time (TE) and the number of excitations (NEX) was set to 5,000 msec, 30 msec and 6, respectively. The volume of interest was set to the left centrum-semiovale (where no

MRI abnormality was seen), which measured 40 mm×25 mm×25 mm (Fig. 2). To note, another ¹H-MRS with longer TE (TR/TE/NEX set to 5,000 msec/135 msec/15) was acquired at the same volume of interest in addition (Fig. 2), as described later.

T2-weighted images and FLAIR images demonstrated slight minimum high-intensity areas around the trigones of the bilateral lateral ventricles, which were hardly distinguishable from the terminal zone (Fig. 1). No other pathological finding was noted in the MRI examination. On the other hand, ¹H-MRS revealed a prominent and narrow abnormal peak at 1.3 ppm and a relatively small narrow peak at 0.9 ppm (Fig. 2). To exclude lactate from the peak at 1.3 ppm, the aforementioned additional ¹H-MRS with longer TE was acquired at the same volume of interest. The peaks at 1.3 ppm and 0.9 ppm remained at this setting (Fig. 2), suggesting that they were derived from lipids, as the peak at 1.3 ppm would have been inverted if it

Fig. 2 MR spectroscopy. **a** Proton MR spectroscopy (¹H-MRS) (TR/TE/NEX=5,000 msec/30 msec/6) and **(b)** ¹H-MRS (TR/TE/NEX=5,000 msec/135 msec/15) both acquired at the same volume of interest at the left centrum-semiovale. Narrow abnormal resonance peaks at 1.3 ppm and 0.9 ppm are demonstrated in both **(a)** and **(b)** (*arrows*). NEX = number of excitations, *NAA* = N-acetyl aspartate, *Cr* = creatine, *Cho* = choline



were derived from lactate. A quantitative analysis based on LCModel was made and lipid peak at 1.3 ppm was confirmed. Other major molecules, including N-acetylaspartate, creatine, myo-inositol and choline, which were all within normal limits, were also confirmed on LCModel. Based on the ^1H -MRS finding, in addition to the clinical symptoms, molecular analysis was conducted for suspicion of SLS.

Molecular analysis

Written informed consent was obtained from the girl's parents. Sequencing of all 11 exons and exon/intron junctions of the ALDH3A2 gene identified two mutations including c.1339A > G (p.K447E) in exon 9 and c.504_505insAG (p.Glu169ArgfsX8) in exon 4 in the heterozygote state, respectively. The first mutation is known as a disease-causing allele, resulting in reduced FALDH activity as low as 1% of normal [4]. The final diagnosis of SLS was made. Of note, the second mutation is a novel mutation of ALDH3A2 not previously described.

Discussion

This case emphasizes the importance and usefulness of ^1H -MRS in diagnosing SLS, since the genetic testing was difficult to be triggered from the mild clinical symptoms and nonspecific MRI findings alone. It is well known that SLS is characterized by unusual narrow and prominent resonance peaks at 1.3 ppm and 0.9 ppm in ^1H -MRS, which correspond to the resonance of lipids. This finding is observed in all SLS cases published to date without exception when ^1H -MRS was acquired from the deep cerebral white matter of the brain [1, 5]. The MRI findings of the present case may be milder than any of the others. Another case of SLS reported by Nakayama et al. [5] also demonstrates mild MRI findings despite the prominent lipid peak on ^1H -MRS, but we presume that the MRI findings of our case are even less notable, especially given that ^1H -MRS in our case was acquired from a region without any MRI abnormalities, compared to the previous case that acquired ^1H -MRS from an area with abnormal high intensity in T2-weighted imaging. Willemsen et al. [1] evaluated ^1H -MRS acquired from 18 SLS patients and reported elevated levels of creatine (+14%), choline (+18%) and myo-inositol (+54%) in addition to lipids, but the molecules other than lipids were not elevated in our case.

The prominent and narrow resonance at 1.3 ppm is where the protons of methylene groups ($-\text{[CH}_2\text{]}_n-$) resonate, while the resonance at 0.9 ppm is where the protons of

methyl groups ($-\text{[CH}_2\text{]}_n-\text{CH}_3$) resonate. These peaks in SLS presumably represent lipids that accumulate because of the FALDH deficiency, which may be fatty alcohols, fatty aldehydes and their metabolites [1]. It may be important to note that the resonance at 1.3 ppm and 0.9 ppm is not specific to SLS. Previous studies reported unusual peaks at 1.3 ppm (and 0.9 ppm) in other pathological states, including peroxisomal diseases such as Zellweger syndrome [6] or rhizomelic chondrodysplasia punctata [7], and other diseases including cerebrotendinous xanthomatosis [8]. In those cases, the lipid peaks are less prominent and broader compared to SLS, and visualized only in a short echo time (e.g., 30 msec) in contrast to SLS, in which peaks are visualized in a longer echo time (135 msec in the presented case). However, we still may not make a diagnosis of SLS based solely on a finding of these abnormal peaks on ^1H -MRS because methylene groups and methyl groups are both quite common structures in organic matters, and many other diseases (including metabolic and storage disorders of higher fatty acids and/or higher hydrocarbon) or conditions of destroyed normal tissue may present similar abnormal peaks.

In patients without typical clinical symptoms or without prominent white matter abnormality on MRI, ^1H -MRS is a useful tool to facilitate an appropriate molecular survey to make a diagnosis of SLS.

References

1. Willemsen MA, Van Der Graaf M, Van Der Knaap MS et al (2004) MR imaging and proton MR spectroscopic studies in Sjogren-Larsson syndrome: characterization of the leukoencephalopathy. *AJNR* 25:649–657
2. Ganemo A, Jagell S, Vahlquist A (2009) Sjogren-larsson syndrome: a study of clinical symptoms and dermatological treatment in 34 Swedish patients. *Acta Derm Venereol* 89:68–73
3. Rizzo WB (2007) Sjogren-Larsson syndrome: molecular genetics and biochemical pathogenesis of fatty aldehyde dehydrogenase deficiency. *Mol Genet Metab* 90:1–9
4. Rizzo WB, Carney G, Lin Z (1999) The molecular basis of Sjogren-Larsson syndrome: mutation analysis of the fatty aldehyde dehydrogenase gene. *Am J Hum Genet* 65:1547–1560
5. Nakayama M, Tavora DG, Alvim TC et al (2006) MRI and ^1H -MRS findings of three patients with Sjogren-Larsson syndrome. *Arq Neuropsiquiatr* 64:398–401
6. Bruhn H, Kruse B, Korenke GC et al (1992) Proton NMR spectroscopy of cerebral metabolic alterations in infantile peroxisomal disorders. *J Comput Assist Tomogr* 16:335–344
7. Viola A, Confort-Gouny S, Ranjeva JP et al (2002) MR imaging and MR spectroscopy in rhizomelic chondrodysplasia punctata. *AJNR* 23:480–483
8. Embirucu EK, Otaduy MC, Taneja AK et al (2010) MR spectroscopy detects lipid peaks in cerebrotendinous xanthomatosis. *AJNR* 31:1347–1349

Frameshift mutation in the *PTCH2* gene can cause nevoid basal cell carcinoma syndrome

Katsunori Fujii · Hirofumi Ohashi ·
Maiko Suzuki · Hiromi Hatsuse · Tadashi Shiohama ·
Hideki Uchikawa · Toshiyuki Miyashita

© Springer Science+Business Media Dordrecht 2013

Abstract Nevoid basal cell carcinoma syndrome (NBCCS) is an autosomal dominant disorder characterized by developmental defects and tumorigenesis. The gene responsible for NBCCS is *PTCH1*, encoding a receptor for the secreted protein, sonic hedgehog. Recently, a Chinese family with NBCCS carrying a missense mutation in *PTCH2*, a close homolog of *PTCH1*, was reported. However, the pathological significance of missense mutations should be discussed cautiously. Here, we report a 13-year-old girl diagnosed with NBCCS based on multiple keratocystic odontogenic tumors and rib anomalies carrying a frameshift mutation in the *PTCH2* gene (c.1172_1173delCT). Considering the deleterious nature of the frameshift mutation, our study further confirmed a causative role for the *PTCH2* mutation in NBCCS. The absence of typical phenotypes in this case such as palmar/plantar pits, macrocephaly, falx calcification, hypertelorism and coarse face, together with previously reported cases, suggested that individuals with NBCCS carrying a *PTCH2* mutation may have a milder phenotype than those with a *PTCH1* mutation.

Keywords Nevoid basal cell carcinoma syndrome · *PTCH1* · *PTCH2* · Frameshift mutation

K. Fujii · T. Shiohama · H. Uchikawa
Department of Pediatrics, Chiba University Graduate School
of Medicine, Chiba 260-8670, Japan

H. Ohashi
Division of Medical Genetics, Saitama Children's Medical
Center, Saitama 339-8551, Japan

M. Suzuki · H. Hatsuse · T. Miyashita (✉)
Department of Molecular Genetics, Kitasato University
Graduate School of Medical Sciences, 1-15-1 Kitasato,
Minami-ku, Sagami-hara 252-0374, Japan
e-mail: tmiyashi@med.kitasato-u.ac.jp

Introduction

Nevoid basal cell carcinoma syndrome (NBCCS) (OMIM 109400), also known as Gorlin syndrome, is an autosomal dominant disorder characterized by developmental defects including bifid ribs, palmar or plantar pits, and tumorigenesis such as the development of basal cell carcinoma, medulloblastoma, or keratocystic odontogenic tumor (KCOT) (formerly known as odontogenic keratocysts) [1]. It is transmitted with complete penetrance and variable expressivity. The gene responsible for NBCCS is the human homologue of the *Drosophila patched* gene, *PTCH1* [2, 3]. The human *PTCH1* gene contains 23 coding exons spanning approximately 70 kb and encodes a protein of 1,447 amino-acid residues containing 12 transmembrane-spanning domains and two large extracellular loops [2]. The *PTCH1* protein is the ligand-binding component of the sonic hedgehog (Shh) receptor complex. In the absence of Shh binding, *PTCH1* is thought to hold smoothed (SMO), a 7-pass transmembrane protein, in an inactive state and thus inhibit signaling to downstream genes. Upon the binding of Shh, the inhibition of SMO is released and signaling is transduced leading to the activation of target genes by the Gli family of transcription factors [4]. Therefore, aberrant activation of the Shh signaling cascade due to the haploinsufficiency of *PTCH1* is believed to cause NBCCS.

In vertebrates, there exists a close homolog of *PTCH1* named *PTCH2*. The human *PTCH2* gene contains 22 coding exons spanning approximately 15 kb and encodes a protein of 1,203 amino-acid residues [5]. Recently, in six affected members of a Chinese Han family with NBCCS, Fan et al. identified a heterozygous germline missense mutation in the *PTCH2* gene [6]. Here we report a case with NBCCS carrying a frameshift mutation due to a 2-bp

deletion in *PTCH2*. To our knowledge, this is the first report of NBCCS caused by a frameshift mutation and the second report of a germline mutation in the *PTCH2* gene.

Clinical report

A 13-year-old Japanese girl was referred to our hospital with jaw cysts and a rib abnormality. She was born weighing 2,570 g, with a height of 48 cm and a head circumference of 32 cm. Her two siblings as well as her parents exhibited no similar features. No consanguineous marriage was noticed in her pedigree. At 10 years of age, she had multiple KCOTs (Fig. 1a) and underwent a surgical operation to remove them. At 12 years of age, she exhibited proteinuria, and was diagnosed as having chronic glomerular nephritis. Then, she was referred to our hospital for further investigation. At examination, she was 150.1 cm tall (mean) and weighed 57.8 kg (+1.8SD). Her head circumference was 54.6 cm (mean). She had normal intelligence without neurological deficit. She exhibited no structural abnormalities of face, oral cavity, or limbs. However, chest roentgenogram revealed a left bifid rib without any other bone abnormalities (Fig. 1b). She did not exhibit palmar or plantar pits, falx calcification, medulloblastomas, or basal cell carcinomas at that time. Since she exhibited KCOTs and a rib anomaly fulfilling the diagnostic criteria made by Kimonis et al. (two major criteria), we diagnosed her as having NBCCS.

Methods

DNA extraction and PCR-sequencing analysis

All experiments described below were approved by the ethics committee at Kitasato University. DNA was extracted from peripheral blood lymphocytes using a QIAamp DNA blood midi kit (QIAGEN). The complete coding region of the *PTCH1*, *PTCH2*, suppressor of fused (*SUFU*) and *SMO* genes, including all splice junctions, was amplified from

constitutional DNA as described previously [7]. Primers used for amplifying *PTCH1*, *PTCH2* and *SUFU* exons were described previously [5, 7, 8]. Those used for amplifying *SMO* are listed in supporting information Table 1. Amplified products were gel-purified using a QIAEX II gel extraction kit (QIAGEN) and cycle sequenced with a BigDye Terminator v3.1 Cycle Sequencing Kit (Applied Biosystems) in both directions. The sequence was analyzed on a 3130 Genetic Analyzer (Applied Biosystems).

Comparison of clinical manifestations

Details of a nationwide survey of NBCCS performed in Japan have been described previously [9]. The survey covered 157 NBCCS patients whose clinical details were available. Major and minor criteria for NBCCS proposed by Kimonis et al. [10] were evaluated in these patients and compared with those observed in patients carrying a *PTCH2* mutation reported previously including the present case [6].

Results

No mutation in *PTCH1* or the related genes *SUFU* and *SMO* was detected in the peripheral blood from this patient. Although deletion of the entire *PTCH1* gene is a common event in point mutation-negative cases of NBCCS as we reported previously [11], no such deletion was observed using either a ligation-dependent probe amplification method or high-resolution array-based comparative genomic hybridization technology [11–13]. We then sequenced all exons of the *PTCH2* gene, since *PTCH2* is a close homolog of *PTCH1* and is also a suppressor component of the Shh pathway. As a result, a heterozygous 2-base-pair deletion, c.1172_1173delCT, was detected in exon 9 of *PTCH2* (Fig. 2). This mutation caused a frameshift and created a premature termination codon (PTC) at the site of the deletion resulting in a truncated form of the PTCH2 protein, p.S391X.

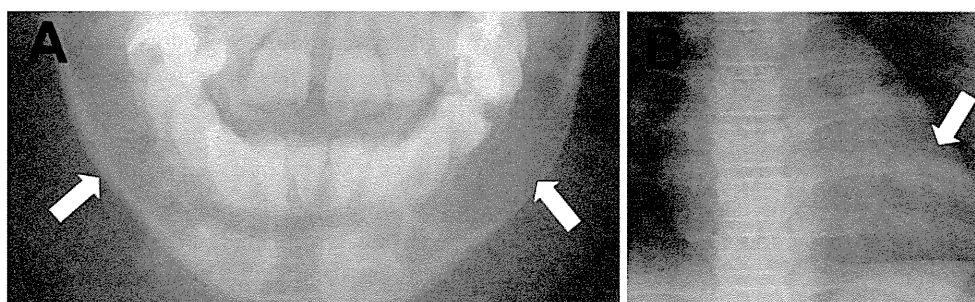


Fig. 1 Roentgenograms of the patient. **a** Pantomography shows bilateral keratocystic odontogenic tumors (Arrows). **b** Chest roentgenogram reveals a bifid anomaly of the left sixth rib (Arrow)

Table 1 Comparison of the characteristic phenotype of NBCCS in three groups

Patients	Number of patients	Mean age	Mean number of major criteria	Mean number of minor criteria
Nationwide survey	157	33.1	2.4*	1.3**
With <i>PTCH2</i> mutation	7	34.1	1.57	0.14

* $P < 0.05$ (vs *PTCH2* mutation), ** $P < 0.01$ (vs *PTCH2* mutation)

In order to characterize the phenotype of individuals carrying a *PTCH2* mutation, we next evaluated the number of positive criteria for NBCCS proposed by Kimonis et al. [10] in two groups; first, NBCCS patients collected by a nationwide survey described previously [9], second, reported individuals carrying a *PTCH2* mutation including our case. In spite of the comparable mean ages in two groups (33.1 vs 34.1 years old), positivities of most of the criteria were lower in the *PTCH2* mutation-positive group than in the other, indicating that *PTCH2* mutations cause a milder phenotype than the classical NBCCS (Table 1). In fact, only 4 out of 7 individuals in the *PTCH2* mutation-positive group diagnosed as having NBCCS according to this diagnostic criteria.

Discussion

NBCCS is caused by a mutation in the gene *PTCH1*, with rare exceptions in which a *SUFU* mutation has been identified [8, 14, 15]. Recently, a heterozygous missense mutation in the *PTCH2* gene, c.2157G>A (p.R719Q), was identified in 6 affected members of a Chinese Han family with NBCCS [6]. Although the pathological significance of missense mutations should be discussed cautiously, this mutation was demonstrated

to result in the inactivation of *PTCH2*'s inhibitory activities at least in vitro. In this paper, we reported a second germline mutation of *PTCH2*, c.1172_1173delCT, found in a Japanese patient with NBCCS. This mutation created a PTC at the site of the deletion in the mutant allele, resulting in the truncation of the *PTCH2* protein. However, since the PTC leads to the degradation of mRNA via a mechanism called nonsense-mediated mRNA decay [16], a haploinsufficiency of *PTCH2* is expected to play an important role in this case.

Interestingly, this mutation is also present in the dbSNP database as rs56126236, submitted by the Center for Genome Medicine, Kyoto University Graduate School of Medicine, Japan. However, details such as frequency are unclear. Therefore, we analyzed 63 healthy Japanese individuals (126 alleles) on this mutation, but found none carrying this deletion. Thus, it is unlikely that this is a rare polymorphism at least in a Japanese population.

However, unfortunately, we were unable to get informed consents from family members and, therefore, could not add data regarding this issue. Nonetheless, considering the deleterious nature of the mutation, we believe that the mutation found in this patient is generated de novo.

Homozygous mutant mice, *Ptch2*^{-/-}, developed normally, were viable and fertile, and did not display any obvious defects in hair follicle, limb, neural, or testis development [17]. However, with age, homozygous mutant male mice developed skin lesions consisting of alopecia and epidermal hyperplasia, suggesting a role for *Ptch2* in adult epidermal homeostasis via Shh signaling. In accordance with the milder phenotype of *Ptch2*^{-/-} than *Ptch1*^{-/-}, which is embryonic lethal [18], it is not surprising that individuals carrying a *PTCH2* mutation also exhibit milder clinical manifestations than those with classical NBCCS. Our patient lacked typical NBCCS phenotypes such as palmar/plantar pits, falx calcification, macrocephaly, hypertelorism and coarse face, the frequencies of which are 60.1, 79.6, 26.5, 68.8, and 27.9 %, respectively, in the Japanese population [9]. In fact, this case does not fulfill the criteria by Evans et al. [19] because a rib anomaly is considered to be a minor criterion. Since the number of cases with a *PTCH2* mutation is still limited, the accumulation of such patients is expected to further clarify their characteristic phenotype.

A genotype–phenotype correlation has not been reported in NBCCS patients [20]. However, mutations in the *SUFU*

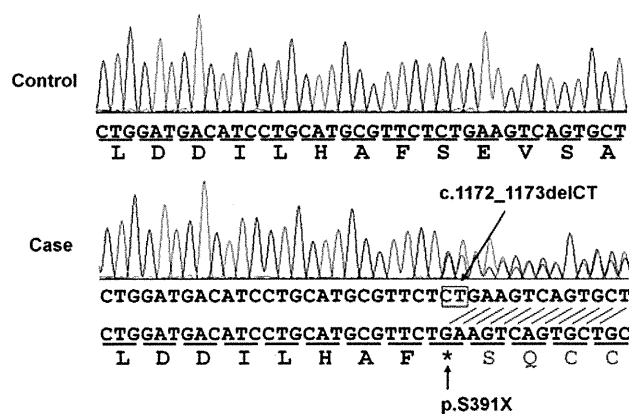


Fig. 2 Electropherograms of the *PTCH2* exon 9 sequence. DNA extracted from the peripheral blood of the patient (Case) as well as a healthy control (Control) was subjected to PCR direct sequencing. The predicted translation is indicated at the bottom of each electropherogram. PTC created by the deletion is indicated by an asterisk

gene were reported to result in a much higher incidence of medulloblastoma than those in *PTCH1* [8, 14, 21]. It is also reported that a large genomic deletion encompassing *PTCH1* leads to NBCCS with atypical clinical manifestations, probably due to a deletion of adjacent gene(s) [12]. Therefore, it should be noted that NBCCS cases caused by a mutation of a gene other than *PTCH1* have phenotypes different from those of classical NBCCS caused by *PTCH1* mutations.

Acknowledgments This research was supported by Science Research Grants for intractable diseases in Japan (H22-intractable diseases-120) from the Ministry of Health, Labour and Welfare, and by a Grant-in-Aid for Scientific Research (20591261) from the Ministry of Education, Culture, Sports, Science and Technology.

Conflict of interest The authors declare that they have no conflict of interest.

References

- Gorlin RJ (1987) Nevoid basal-cell carcinoma syndrome. *Medicine* (Baltimore) 66:98–113
- Johnson RL, Rothman AL, Xie J, Goodrich LV, Bare JW, Bonifas JM, Quinn AG, Myers RM, Cox DR, Epstein EH Jr, Scott MP (1996) Human homolog of *patched*, a candidate gene for the basal cell nevus syndrome. *Science* 272:1668–1671
- Hahn H, Wicking C, Zaphiropoulos PG, Gailani MR, Shanley S, Chidambaram A, Vorechovsky I, Holmberg E, Uden AB, Gillies S, Negus K, Smyth I, Pressman C, Leffell DJ, Gerrard B, Goldstein AM, Dean M, Toftgard R, Chenevix-Trench G, Wainwright B, Bale AE (1996) Mutations of the human homolog of *Drosophila patched* in the nevoid basal cell carcinoma syndrome. *Cell* 85:841–851
- Ingham PW, McMahon AP (2001) Hedgehog signaling in animal development: paradigms and principles. *Genes Dev* 15:3059–3087
- Smyth I, Narang MA, Evans T, Heimann C, Nakamura Y, Chenevix-Trench G, Pietsch T, Wicking C, Wainwright BJ (1999) Isolation and characterization of human *patched 2* (*PTCH2*), a putative tumour suppressor gene in basal cell carcinoma and medulloblastoma on chromosome 1p32. *Hum Mol Genet* 8:291–297
- Fan Z, Li J, Du J, Zhang H, Shen Y, Wang CY, Wang S (2008) A missense mutation in *PTCH2* underlies dominantly inherited NBCCS in a Chinese family. *J Med Genet* 45:303–308
- Fujii K, Kohno Y, Sugita K, Nakamura M, Moroi Y, Urabe K, Furue M, Yamada M, Miyashita T (2003) Mutations in the human homologue of *Drosophila patched* in Japanese nevoid basal cell carcinoma syndrome patients. *Hum Mutat* 21:451–452
- Kijima C, Miyashita T, Suzuki M, Oka H, Fujii K (2012) Two cases of nevoid basal cell carcinoma syndrome associated with meningioma caused by a *PTCH1* or *SUFU* germline mutation. *Fam Cancer* 11:565–570
- Endo M, Fujii K, Sugita K, Saito K, Kohno Y, Miyashita T (2012) Nationwide survey of nevoid basal cell carcinoma syndrome in Japan revealing the low frequency of basal cell carcinoma. *Am J Med Genet A* 158A:351–357
- Kimonis VE, Goldstein AM, Pastakia B, Yang ML, Kase R, DiGiovanna JJ, Bale AE, Bale SJ (1997) Clinical manifestations in 105 persons with nevoid basal cell carcinoma syndrome. *Am J Med Genet* 69:299–308
- Nagao K, Fujii K, Saito K, Sugita K, Endo M, Motojima T, Hatsuse H, Miyashita T (2011) Entire *PTCH1* deletion is a common event in point mutation-negative cases with nevoid basal cell carcinoma syndrome in Japan. *Clin Genet* 79:196–198
- Fujii K, Ishikawa S, Uchikawa H, Komura D, Shapero MH, Shen F, Hung J, Arai H, Tanaka Y, Sasaki K, Kohno Y, Yamada M, Jones KW, Aburatani H, Miyashita T (2007) High-density oligonucleotide array with sub-kilobase resolution reveals breakpoint information of submicroscopic deletions in nevoid basal cell carcinoma syndrome. *Hum Genet* 122:459–466
- Kosaki R, Nagao K, Kameyama K, Suzuki M, Fujii K, Miyashita T (2012) Heterozygous tandem duplication within the *PTCH1* gene results in nevoid basal cell carcinoma syndrome. *Am J Med Genet A* 158A:1724–1728
- Taylor MD, Liu L, Raffel C, Hui CC, Mainprize TG, Zhang X, Agatep R, Chiappa S, Gao L, Lowrance A, Hao A, Goldstein AM, Stavrou T, Scherer SW, Dura WT, Wainwright B, Squire JA, Rutka JT, Hogg D (2002) Mutations in *SUFU* predispose to medulloblastoma. *Nat Genet* 31:306–310
- Pastorino L, Ghiorzo P, Nasti S, Battistuzzi L, Cusano R, Marzocchi C, Garre ML, Clementi M, Scarra GB (2009) Identification of a *SUFU* germline mutation in a family with Gorlin syndrome. *Am J Med Genet A* 149A:1539–1543
- Holbrook JA, Neu-Yilik G, Hentze MW, Kulozik AE (2004) Nonsense-mediated decay approaches the clinic. *Nat Genet* 36:801–808
- Nieuwenhuis E, Motoyama J, Barnfield PC, Yoshikawa Y, Zhang X, Mo R, Crackower MA, Hui CC (2006) Mice with a targeted mutation of *patched2* are viable but develop alopecia and epidermal hyperplasia. *Mol Cell Biol* 26:6609–6622
- Goodrich LV, Milenkovic L, Higgins KM, Scott MP (1997) Altered neural cell fates and medulloblastoma in mouse *patched* mutants. *Science* 277:1109–1113
- Evans DG, Ladusans EJ, Rimmer S, Burnell LD, Thakker N, Farndon PA (1993) Complications of the nevoid basal cell carcinoma syndrome: results of a population based study. *J Med Genet* 30:460–464
- Wicking C, Shanley S, Smyth I, Gillies S, Negus K, Graham S, Suthers G, Haites N, Edwards M, Wainwright B, Chenevix-Trench G (1997) Most germ-line mutations in the nevoid basal cell carcinoma syndrome lead to a premature termination of the *PATCHED* protein, and no genotype–phenotype correlations are evident. *Am J Hum Genet* 60:21–26
- Brugieres L, Pierron G, Chompret A, Paillerets BB, Di Rocco F, Varlet P, Pierre-Kahn A, Caron O, Grill J, Delattre O (2010) Incomplete penetrance of the predisposition to medulloblastoma associated with germ-line *SUFU* mutations. *J Med Genet* 47:142–144

CASE REPORT

Patient with terminal 9 Mb deletion of chromosome 9p: Refining the critical region for 9p monosomy syndrome with trigonocephaly

Norimasa Mitsui¹, Kenji Shimizu², Hiroshi Nishimoto³, Hiroshi Mochizuki⁴, Masao Iida¹, and Hirofumi Ohashi²

¹Department of Clinical Laboratory, Divisions of ²Medical Genetics, ³Neurosurgery, and ⁴Metabolism and Endocrinology, Saitama Children's Medical Center, Saitama, Japan

ABSTRACT We describe a patient with typical manifestations of 9p monosomy syndrome, including trigonocephaly and sex reversal. Array comparative genomic hybridization (CGH) revealed a 9p terminal deletion of approximately 9 Mb with the breakpoint at 9p23. We compared the deleted segments of 9p associated with reported cases of 9p monosomy syndrome with trigonocephaly. We did not identify a region that was shared by all patients; however, when only pure terminal or interstitial deletions that did not involve material from any other chromosome were compared, we identified a segment from D9S912 to RP11-439I6 of approximately 1 Mb that was deleted in every patient. We propose that this 1-Mb segment might be the critical region for 9p monosomy syndrome with trigonocephaly.

Key Words: 9p monosomy, craniosynostosis, critical region, sex reversal, trigonocephaly

INTRODUCTION

Monosomy 9p syndrome [MIM 158170] is a rare but well-known chromosomal deletion syndrome characterized by distinct craniofacial features (including trigonocephaly), various systemic anomalies, developmental retardation, and occasional sex reversal in XY patients (Huret et al. 1988). Since Alfi et al. (1973) first described a patient with the syndrome, more than 100 patients, most with terminal deletions with breakpoints around 9p21-p23 based on chromosome G-band analysis, have been reported. Recent advances in molecular/cytogenetic techniques allow attempts to map the loci responsible for cardinal features of the syndrome, especially trigonocephaly and sex reversal. While *DMRT* genes, which map to the most terminal 9p24.3 band, have been elucidated as the genes responsible for sex reversal (Raymond et al. 1998; Ogata et al. 2001; Barbaro et al. 2009), no gene has yet been identified as definitively responsible for trigonocephaly. Moreover, previous studies have been inconsistent with regard to identification of the 9p regions that are responsible for trigonocephaly (Wagstaff and Hemann 1995; Christ et al. 1999; Kawara et al. 2006; Faas et al. 2007; Hauge et al. 2008; Swinkels et al. 2008; Shimojima and Yamamoto 2009). Here, we describe a patient with a terminal 9p deletion of approximately 9 Mb who has the typical clinical manifestations of 9p monosomy syndrome, including trigonocephaly and sex reversal.

CLINICAL REPORT

The girl patient was born by cesarean section after 38-week gestation to a 30-year-old gravida 2, para 1 mother and a 31-year-old father, both Japanese, healthy, and unrelated. The patient's birth weight was 2864 g (−0.5 SD), length 49.5 cm (+0.2 SD), and occipitofrontal head circumference 35.5 cm (+1.5 SD). The patient had a healthy older sister. The patient was referred to us at the age of 11 months because of developmental delay and skull deformity. The notable craniofacial features were trigonocephaly, ptosis of the eyelids, epicanthus, upslanting palpebral fissures, flat nasal bridge, broad nasal root, long philtrum, thin upper lip, and low-set ears. A skull computed tomography scan with 3D reconstruction confirmed trigonocephaly with metopic suture synostosis (Fig. 1). Fronto-orbital advancement with cranial reshaping was performed when she was 1 year and 3 months old. She showed normal female external genitalia. When the patient was 2 years old, an abdominal ultrasonography revealed a uterus, but no ovary or testis was detected. A test of human chorionic gonadotropin load suggested the existence of testis, while luteinizing hormone-releasing hormone load test revealed primary hypogonadism. She weighed 14 kg (−1.7 SD) and was 100.2 cm tall (−1.9 SD) at 5 years of age. Her development was moderately delayed, and her IQ was estimated to be around 40 with the Tanaka–Binet Intelligence Scale at the age of 6 years.

G-banding analysis at a resolution of 550-bands on metaphase chromosomes obtained from phytohemagglutinin-stimulated lymphocyte cultures from the patient revealed a distal deletion of the short arm of chromosome 9 with a breakpoint at 9p23 and an XY sex chromosome constitution (sex reversal) (Fig. 2). Her parents were chromosomally normal. Fluorescence *in situ* hybridization (FISH) using whole-chromosome painting probes for chromosome 9 and a subtelomeric probe for the short arm of chromosome 9 (both from Vysis/Abbott Molecular Inc., Des Plaines, IL, USA) revealed that the abnormal chromosome 9 did not contain translocated material from another chromosome. To further define the extent of the deleted region in 9p, we performed an array comparative genomic hybridization (CGH) analysis using the Agilent Human Genome 244 K CGH kit (Agilent Technologies, Santa Clara, CA, USA). The result showed a hemizygous 9.17 Mb terminal deletion of chromosome 9p and no other apparent pathogenic copy number variation was identified in the whole genome (Fig. 3). Her karyotype was designated as 46,XY,del(9)(p23).arr 9p23 (194 193-9 169 072)x1 dn. FISH analyses with bacterial artificial chromosome (BAC) clones spanning the region from 9p23 to 9p24 refined the breakpoint between the clones RP11-1134E16 (D9S2000) and RP11-74 L16 (D9S912) (Table 1). BACs containing *DMRT1* and *DMRT2*, both candidate genes for sex reversal (9p24.3), were confirmed to be in the deleted segment of 9p in the patient.

Correspondence: Hirofumi Ohashi, MD, PhD, Division of Medical Genetics, Saitama Children's Medical Center, 2100 Magome, Iwatsuki-ku, Saitama-shi, Saitama 339-8551, Japan. Email: ohashi.hirofumi@pref.saitama.lg.jp

Received January 20, 2012; revised and accepted February 9, 2012.

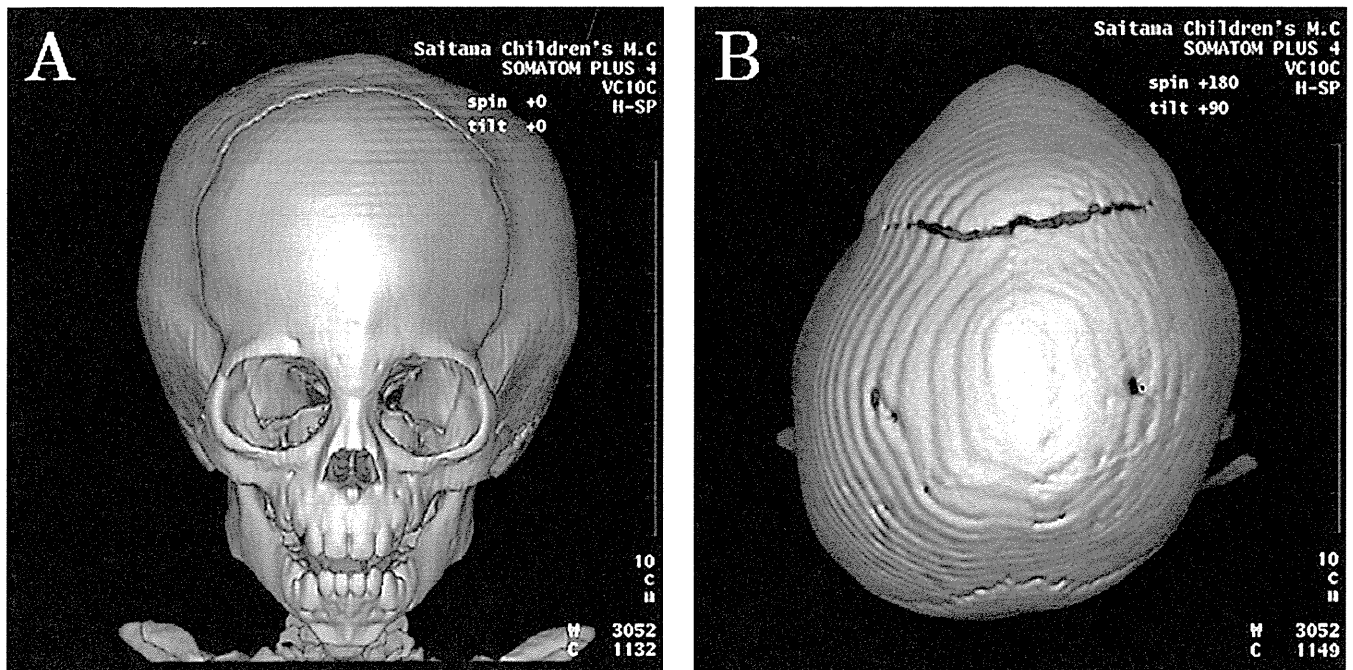


Fig. 1 Frontal (a) and top (b) views of the skull of the patient at age 11 months showing trigonocephaly, reconstructed by three-dimensional computed tomography.

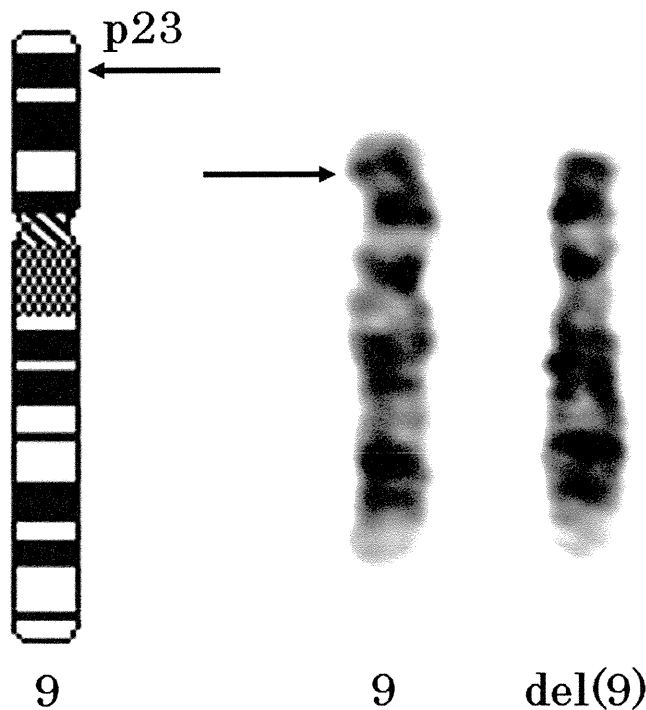


Fig. 2 G-banded partial karyotype of the patient showing a terminal deletion of chromosome 9. Arrow indicates the deletion breakpoint.

DISCUSSION

We described herein a girl patient with a terminal deletion of the short arm of chromosome 9 who had full manifestations of mono-

somy 9p syndrome, including distinctive craniofacial features (e.g. trigonocephaly, ptosis of the eyelids, epicanthus, upslanting palpebral fissures, flat nasal bridge, broad nasal root, low-set ears, long philtrum, thin upper lip), developmental delay, and XY sex reversal. Array CGH and FISH analyses revealed a pure terminal 9p deletion of approximately 9 Mb with the breakpoint between RP11-1134E16 and RP11-74 L16 at 9p23. *DMRT* genes, candidates for sex reversal (9p24.3), were included in the deletion in this patient.

Since Alfi et al. (1973) first reported 9p monosomy syndrome it has been established as a chromosomal deletion syndrome on the basis of G-banding cytogenetic analysis. Breakpoints in most patients with the syndrome, either with a pure terminal deletion or with a deletion associated with an unbalanced chromosome segment, reside around band 9p21-p23 (Huret et al. 1988). Recent advances in molecular techniques have allowed us to study precise correlations between the phenotype and karyotype/genotype associated with this syndrome. Wagstaff and Hemann (1995) first defined the critical region for 9p monosomy syndrome, including trigonocephaly, based on a boy with cryptic 9p monosomy, who was found to have a 9p deletion of approximately 11.6 Mb that included the region from D9S286 (9p24.1) to D9S162 (9p22.1); this deletion was associated with a translocation between 3p and 9p. Christ et al. (1999) studied 24 patients with 9p deletions (terminal deletions with or without unbalanced translocation), all of whom showed the consensus 9p-deletion phenotype (including trigonocephaly), and found that the minimum common deleted region is 16.1 Mb from D9S285 to the 9p terminal. Subsequently, several reports have been published that further define the critical region for the syndrome (Kawara et al. 2006; Faas et al. 2007; Hauge et al. 2008; Swinkels et al. 2008; Shimojima and Yamamoto 2009). Although, along with these works, some genes such as *CER1*, *TYRP1* and *PTPRD* have been postulated as possible candidate genes, no gene has yet been identified as conclusively responsible for the syndrome (Shimojima and Yamamoto 2009).